

Thermal transmittance in graphene based networks for polymer matrix composites

Original

Thermal transmittance in graphene based networks for polymer matrix composites / Bigdeli, Masoud Bozorg; Fasano, Matteo. - In: INTERNATIONAL JOURNAL OF THERMAL SCIENCES. - ISSN 1290-0729. - ELETTRONICO. - 117:(2017), pp. 98-105. [10.1016/j.ijthermalsci.2017.03.009]

Availability:

This version is available at: 11583/2671725 since: 2017-05-23T11:19:04Z

Publisher:

Elsevier Masson SAS

Published

DOI:10.1016/j.ijthermalsci.2017.03.009

Terms of use:

This article is made available under terms and conditions as specified in the corresponding bibliographic description in the repository

Publisher copyright

(Article begins on next page)

Thermal transmittance in graphene based networks for polymer matrix composites

Masoud Bozorg Bigdeli^b, Matteo Fasano^{a,*}

^a*Energy Department, Politecnico di Torino, Corso Duca degli Abruzzi 24, Torino, 10129, Italy*

^b*Department of Mechanical Engineering, University of Alberta, Edmonton, T6G 2G8, Canada*

Abstract

Graphene nanoribbons (GNRs) can be added as fillers in polymer matrix composites for enhancing their thermo-mechanical properties. In the present study, we focus on the effect of chemical and geometrical characteristics of GNRs on the thermal conduction properties of composite materials. Configurations consisting of single and triple GNRs are here considered as representative building blocks of larger filler networks. In particular, GNRs with different length, relative orientation and number of cross-linkers are investigated. Based on results obtained by Reverse Non-equilibrium Molecular Dynamics simulations, we report correlations relating thermal conductivity and thermal boundary resistance of GNRs with their geometrical and chemical characteristics. These effects in turn affect the overall thermal transmittance of graphene based networks. In the broader context of effective medium theory, such results could be beneficial to predict the thermal transport properties of devices made of polymer matrix composites, which currently find application in energy, automotive, aerospace, electronics, sporting goods, and infrastructure industries.

Keywords: Polymer matrix composites, Graphene, Thermal transmittance, Kapitza resistance, Molecular dynamics

*Corresponding author

Email address: matteo.fasano@polito.it (Matteo Fasano)

1. Introduction

Polymer matrix composites (PMCs) have been manufactured to improve the effective thermal, mechanical and electrical properties of pure polymeric materials [1, 2, 3]. The benefits of PMCs, such as light weight, ease of process, high strength, durability, and multifunctionality, have been clearly shown in aerospace applications. In the near future, PMCs are going to be largely exploited in the exponentially rising industry of flexible electronics, as well as in the energy, automotive, aerospace, sporting goods and infrastructure sectors [4, 5, 6].

Among the various filler materials of current engineering interest, carbon based fillers (e.g. graphene, graphene nanoribbons carbon nanotubes) have received increasing attention due to their superior properties, for instance high electrical conductivity, shielding ability, transparency, flexibility, electromagnetic interference, low thermal expansion, mechanical stiffness [7, 8], large thermal conductivity [9, 10], and selective mass transport [11, 12, 13]. Instead, the low thermal conductivities of common polymers ($\approx 0.2 - 0.5 \text{ W/mK}$) have been always a technological limit for industrial applications such as heat exchangers, thermal energy storage systems, electronic systems and machinery [14, 15]. Therefore, the introduction of highly conductive fillers in thermally insulating polymers is expected to enhance the overall thermal and mechanical properties of the resulting polymer matrix composites by some orders of magnitude [4, 16, 17].

However, two main limitations are currently slowing down a more widespread exploitation of such carbon based composites: a weak fiber-matrix adhesion, which typically leads to a progressive degradation of the initial properties; poor out-of-plane properties, due to the anisotropic nature of nanotube or graphene nanofillers. Furthermore, experimental observations and molecular simulations of carbon based networks reveal effective thermal performance lower than expected by traditional effective medium theories [18]. In fact, researchers have realized that, along with the properties of the matrix and the filler, other factors are significantly affecting the overall thermal properties of PMCs, such as

filler distribution (morphology), filler size, filler-matrix and filler-filler interfacial characteristics.

While it is now accepted that the Kapitza resistance at the filler-filler and filler-polymer interfaces presents a major barrier to conductive thermal transport in graphene based polymer matrix composites, a mechanistic understanding of the thermal transport across such interfaces is still missing [18, 19, 20]. Kapitza resistance in PMCs mainly arises from two effects, namely the scattering at the interface between two phases, and the differences between phonon spectra of different phases. An important factor in thermal transport of carbon based PMCs is the heat transport through percolation chains of fillers [21]. Carbon based fillers often fail to form such a network and, as a result, the effective thermal conductivity of the composite material is lower than expected [22].

A possible way to overcome this limitation is cross-linking graphene sheets, e.g. by means of covalent carbon bonds or short polymer chains. In fact, surface chemical functionalization is considered as a promising route to affect thermal, mechanical and electrical properties of composite materials made of carbon based fillers. Hence, the functionalization of fibers has emerged as a particularly interesting field of research, to improve both durable multifunctionality and out-of-plane characteristics of carbon based materials [23]. For example, Worsley *et al.* [24] presented a method for synthesizing graphene aerogels with high electrical conductivities by introducing covalent carbon bonding between contiguous graphene sheets. According to previous studies, even a limited cross-linking could significantly reduce the thermal boundary resistance between carbon based nanostructures, therefore improving the overall thermal transmittance of the composite material [25, 26].

Due to the difficulties encountered in the experimental characterization of graphene based structures with atomistic precision, computational studies have been widely conducted to analyze thermal transport across graphene interfaces. For example, Mortazavi *et al.* [27] investigated the thermal boundary resistance (R_k) between graphene and epoxy matrix by means of molecular dynamics simulations; their results showed that R_k varies from 3.14×10^{-8} to 9.26×10^{-8}

m²K/W depending on the interfacial pressure and cross-linking percentage. Konatham and Striolo [28], instead, studied the thermal boundary resistance at the graphene-oil interface. Their MD simulations revealed that R_k ranges from 3.7×10^{-9} to 4×10^{-8} m²K/W according to the number of functional groups on the edges of graphene sheets.

In the present study, Reverse Non-equilibrium Molecular Dynamics (RNEMD) simulations are performed to clarify the contribution of filler size and filler-filler interfacial thermal resistance (also known as Kapitza resistance or thermal boundary resistance, R_k) to the thermal transmittance within PMCs. Such results are then adopted in the broader context of effective medium theory, in order to provide design guidelines for the thermal transport properties of polymer matrix composites. The multiscale simulation approach discussed in this work may find application in energy, automotive, aerospace, electronics, sporting goods and infrastructure industries.

2. Methods

Both functionalization and geometry of carbon nanotube [25, 29], graphene or graphene nanoribbon (GNR) [30, 31] fillers are responsible of thermal boundary resistance at filler-filler and filler-matrix interfaces. In this work, the attention is focused on the effect of functionalization and geometry (relative orientation, size of fillers) on the R_k at the filler-filler interface, being one of the most critical bottlenecks in the heat transport through the composites. As a case study, here we focus the analyses on GNR fillers. In fact, the thermal conductance per unit width of GNR is higher than graphene one [32] and, thus, GNRs are ideal fillers for composite materials with enhanced heat dissipation properties. However, because of the similar nature of heat transfer also through graphene or carbon nanotube networks, the obtained design guidelines may be considered as generally valid also with other carbon fillers. Configurations consisting of single and triple GNRs are therefore considered as

representative building blocks of larger networks of fillers within PMCs. The thermal transport through armchair-edged graphene nanoribbons is then investigated by reverse non-equilibrium molecular dynamics simulations. More specifically, thermal conductivity and thermal boundary resistance are computed in the considered GNR configurations.

The adopted simulation approach is based on Muller-Plathe's method, where a fixed heat flux is forced from the center of the simulated systems to its extremities, in order to induce a temperature gradient through the system and thus extract thermal properties [33]. The heat flux is generated by continuously exchanging the velocity of the "coldest" atom in the hot slab (v_{cold} , red region in Fig. 1a) with the one of the "hottest" atom in the cold slabs (v_{hot} , blue regions in Fig. 1a). Hence, an artificial energy flux is forced from cold to hot regions by the Muller-Plathe's algorithm. Since energy is conserved in the simulated systems at the steady state, an opposite physical heat flux (j_x) is then induced from hot to cold regions by heat conduction (Fig. 1a), namely

$$j_x = \frac{1}{2tA_{yz}} \sum_{transfers} \frac{m}{2}(v_{hot}^2 - v_{cold}^2), \quad (1)$$

where t is the simulation time, A_{yz} is the cross-sectional area perpendicular to the heat flux direction and m is the atomic mass.

In the molecular dynamics (MD) simulations herein carried out, the adaptive intermolecular reactive empirical bond order (AIREBO) potential implemented in the LAMMPS package is used to describe the reactive, covalent bonding interactions; whereas the nonbonded interactions between GNRs, which are mainly due to van der Waals interactions, are modeled by Lennard-Jones (L-J) potential [34, 35]. The adopted force field is particularly tailored to simulate thermal properties of graphene in a broad variety of configurations [36, 37, 38].

After an initial energy minimization, the MD system is thermalized in the canonical ensemble (NVT). Thereafter, the heat flux is imposed through the system by Muller-Plathe's method, and the system is simulated in the micro-canonical ensemble (NVE) with a time step of 0.5 fs. After that steady temperature profile and heat flux are achieved in the system, simulations are continued up to 2

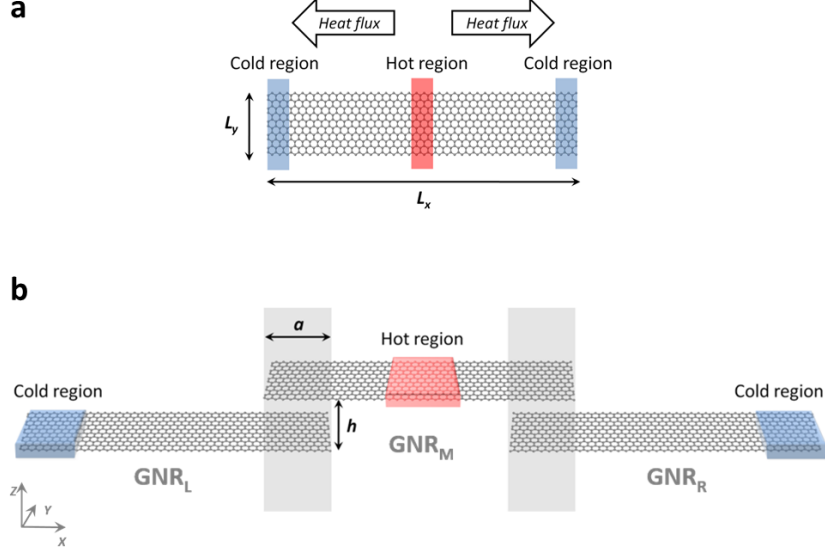


Figure 1: Configurations of GNR fillers studied by atomistic RNEMD simulations. (a) Simulated heat flux through a GNR for evaluating the thermal conductivity of GNRs with different length. (b) Schematic of a triple GNR setup, simulated for investigating the thermal boundary resistance between contiguous GNRs.

ns to guarantee reliable statistics.

GNRs with different lengths (i.e. $L_x = 20, 60, 100, 1000$ nm) and fixed width ($L_y \cong 2.4$ nm) are simulated to study the effect of size on thermal conductivity. In addition, a novel setup for calculating thermal boundary resistance between GNRs using RNEMD method is considered (i.e. triple GNRs), as sketched in Fig. 1b. In this setup, each GNR consists of 1968 carbon atoms and it has $2.4 \text{ nm} \times 20 \text{ nm}$ dimensions, being L_y equal to the perimeter of an armchair (5,5) single wall carbon nanotube. On the one hand, the horizontal overlap (a) and the vertical normal distance (h) between each pair of GNRs are fixed to $a = 4$ nm and $h = 0.25$ nm to investigate the effect of cross-linkers on R_k , because of the geometry of carbon cross-linkers. On the other hand, a and h are freely varied when the effect of relative orientation between fillers on R_k is explored.

3. Results

3.1. Thermal conductivity

Thermal conductivity of GNRs with lengths ranging from 20 to 1000 nm and width fixed to 2.4 nm is then calculated by MD simulations. These dimensions are in the range of both modeling [39, 40] and experimental [41, 42] studies in the literature, which recently focused the attention on graphene nanoribbons with sub-10-nanometers widths. The simulation box is divided into slabs along x -axis, with an approximate linear density of 3 slabs per nanometer. As an example, the 20 nm long GNR is divided into 60 slabs, where the first and the last slabs are the cold regions in the RNEMD procedure, while the 31st is the hot one. Therefore, a temperature gradient (dT/dx) is generated in the system (see Fig. 2), and the thermal conductivity (λ) can be calculated according to Fourier's law:

$$\lambda = -\frac{j_x}{\frac{dT}{dx}}. \quad (2)$$

In Fig. 2, the non-linearity of the temperature profile at the cold and hot regions is due to finite size effects [43], which eventually manifest when the nanostructure length is smaller than the phonon mean free path (MFP) [44].

The results reported in Fig. 3 show that thermal conductivity increases with GNR length, at least up to 1000 nm. In particular, $\lambda \sim L_x^\alpha$ with a best fitted exponent $\alpha \cong 0.48$, which falls within the range predicted by similar studies on graphene and carbon nanotubes [37, 45, 46]. In all simulated cases, thermal conductivity converged to a constant value within the elapsed simulation time: for instance, the convergence of thermal conductivity for the GNR with 1000 nm length is presented in Fig. A1.

Simulation results predict that the GNR length has a significant effect on its thermal conductivity, at least for the considered sub-micrometer lengths. This implies that the thermal conductivity of nanometric GNR fillers does not correspond to the bulk thermal conductivity of graphene, being limited by the

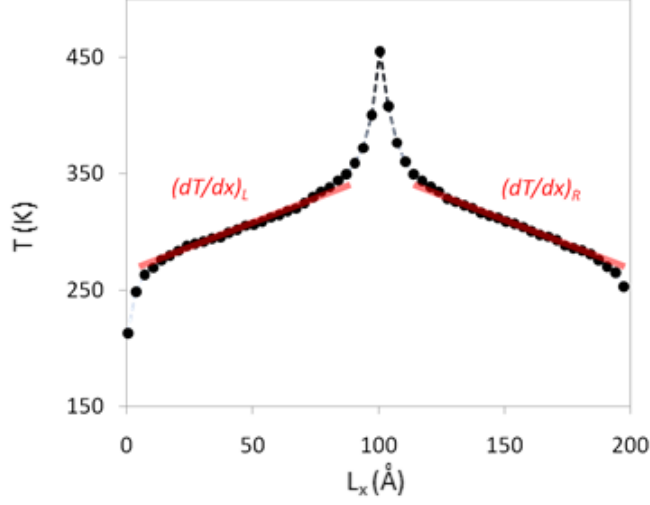


Figure 2: Temperature distribution along a 20 nm GNR during a RNEMD simulation.

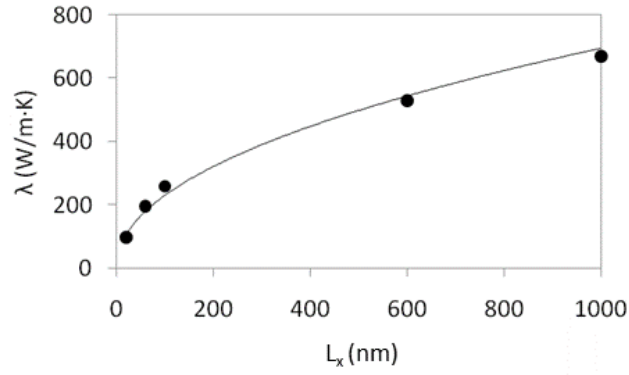


Figure 3: Thermal conductivity (λ) variation for GNRs with different lengths.

finite length of the nanostructure [44]. In fact, the experimental phonon mean free path in graphene is relatively long (775 nm) [47]. Therefore, the thermal conductivity of fillers increases with size for lengths much smaller than MFP, whereas it is expected to be size-invariant for larger dimensions [14, 48, 49, 50].

3.2. Kapitza resistance

The thermal transport through a network of carbon fillers is typically limited by the poor conduction between adjacent fillers, rather than by the thermal conduction of filler themselves. In fact, the carbon fillers used to enhance the thermal properties of polymeric materials often fail to form interconnected networks, and thus their interactions are only governed by weak van der Waals forces [51]. Consequently, the heat transfer is reduced at the filler-filler interface, and thus the resulting thermal conductivity enhancement of the composite is limited.

Since C-C covalent bonds have an interaction potential two orders of magnitude higher than the nonbonded interactions between graphene sheets (i.e., 5.9 eV vs. 50 meV [52, 53]), filler-filler phonon transfer can be generally improved by introducing chemical bonds at their interface. Among other examples in the literature [54, 55], Tian and colleagues experimentally demonstrated the positive impact of covalent interconnects between single-walled carbon nanotubes on the overall electric conduction of a thin film nanotube network [56]. Starting from these experimental evidences, a different amount of carbon cross-linkers between graphene nanoribbons is here simulated as illustrative case. Such covalent joints are the shortest chemically possible between GNRs, therefore guaranteeing the best heat transfer performances through the GNR network.

The thermal boundary resistance between a couple of adjacent fillers can be then evaluated as

$$R_k = -\frac{\Delta T}{j_x}, \quad (3)$$

namely as the temperature jump (ΔT) related to the specific heat flux (j_x) transmitted through the interface [57]. In this study, equation 3 is adopted to calculate the thermal boundary resistance at various GNR-GNR interfaces from ΔT and j_x mechanistically measured by the molecular dynamics experiments.

Let us consider the triple GNRs setup depicted in Fig. 1b, which consists of 3 GNRs located in the left (GNR_L), middle (GNR_M) and right (GNR_R) part of the nanostructure, as a representative building block of GNR networks in

PMCs. In Fig. 4, $\Delta T_{0C,L}$ and $\Delta T_{3C,L}$ are the temperature discontinuities at the GNR_L-GNR_M interface with 0 and 3 carbon cross-linkers, respectively. On the other hand, $\Delta T_{0C,R}$ and $\Delta T_{3C,R}$ indicate the temperature jumps at GNR_M-GNR_R interface with 0 and 3 cross-linkers, respectively.

Knowing the imposed heat flux and resulting temperature distribution along

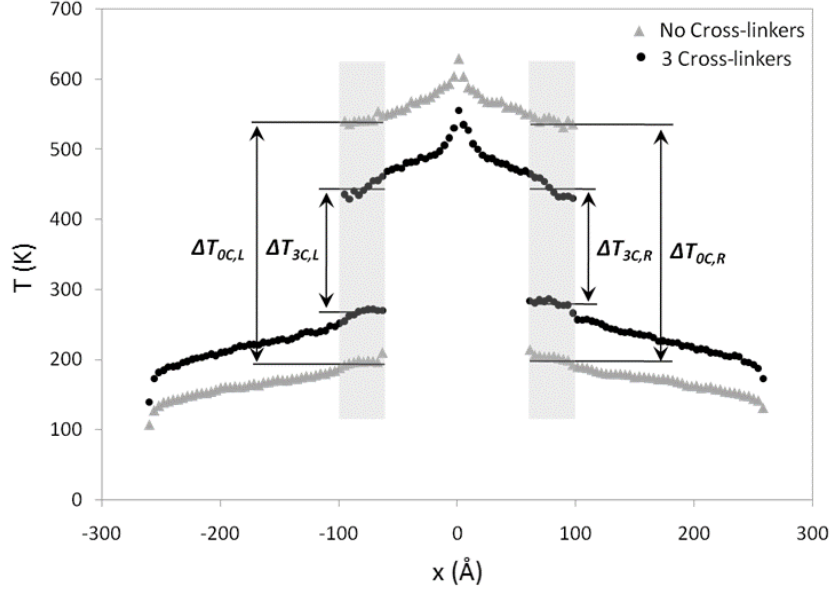


Figure 4: Temperature profile associated with triple GNRs setups with 0 (gray triangles) and 3 (black circles) cross-linkers.

the triple GNR setup, equation 3 allows computing the thermal boundary resistance in triple GNRs setups with $N_{CL} = 0, 1, 2$ and 3 cross-linkers between each pair of overlapping GNRs. To allow a better comparison with experiments, the number of cross-linkers can be normalized by the interface extension ($a \cdot h$), namely $\rho_{CL} = \frac{N_{CL}}{a \cdot h}$, where ρ_{CL} is defined as the surface density of cross-linkers. Simulation results show that, by introducing 3 cross-linkers, the imposed heat flux by RNEMD method increases from 4×10^{11} to 5.3×10^{11} W/m² respect the case without covalent bonds between GNRs, while the resulting temperature jump at the interface decreases from 360 to 180 K.

According to equation 3, these trends lead to a decreasing thermal boundary resistance between overlapping GNRs (Fig. 5), namely from $9.0 \times 10^{-10} \text{ m}^2\text{K/W}$ (0 joints) to $3.4 \times 10^{-10} \text{ m}^2\text{K/W}$ (3 joints). Note that, in all the simulated cases, Kapitza resistances converge to constant values within the elapsed simulation time (see for example Fig. A2). Hence, results show that thermal boundary resistance between overlapping GNRs tends to decrease with ρ_{CL} , namely with the surface density of cross-linkers. Similarly to previous studies [25, 29], the decreasing trend of R_k can be accurately ($R^2=0.98$) fitted by a semi-empirical exponential equation:

$$R_k = R_{k,\rho_0} \exp(\alpha_\rho \rho_{CL}), \quad (4)$$

where $R_{k,\rho_0} = 9.0 \times 10^{-10} \text{ m}^2\text{K/W}$ is the Kapitza resistance with no cross-linkers, and $\alpha_\rho = -3.09 \text{ nm}^2$ (see Fig. 5).

The relation between thermal boundary resistance and overlap or normal dis-

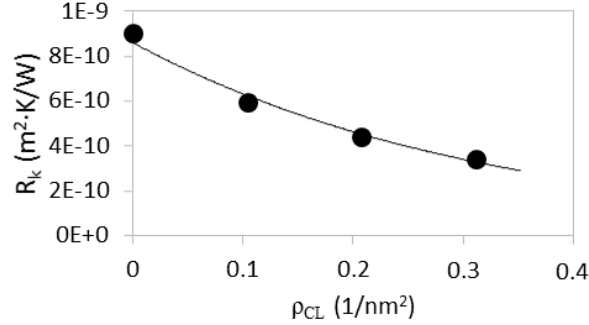


Figure 5: Thermal boundary resistance (R_k) at the GNR-GNR interface as a function of the surface density (ρ_{CL}) of cross-linkers between contiguous nanoribbons. Molecular dynamics results (black dots) are fitted by the correlation reported in equation 4 (black curve).

tance at fiber-fiber interface is then investigated, to obtain a more mechanistic derivation of R_{k,ρ_0} . In detail, the effect of horizontal overlap, a , is studied by simulations performed over the range 20–80 Å, while keeping a fixed normal distance between GNRs ($h_0 = 4 \text{ Å}$) and no cross-linkers. Results in Fig. 6a show an exponential decrease of R_{k,ρ_0} with the increasing overlap, because of

the larger GNR-GNR interface. Moreover, the effect of vertical spacing, h , is studied over the range 2.5–8 Å (constant $a_0 = 40$ Å). In this case, results in Fig. 6b show a direct exponential relation between R_{k,ρ_0} and h , because of decreasing nonbonded interactions (and thus energy transport) with larger relative distances between GNRs. Note that these observations are in qualitative agreement with previously reported results [31]. To provide a quantitative correlation between R_{k,ρ_0} and the geometrical characteristics of the GNR network, the simulation results reported in Fig. 6 are fitted ($R^2=0.94$) in the considered simulation range by the exponential equation

$$R_{k,\rho_0} = R_{k,(\rho_0,h_0,a_0)} \exp [\alpha_a (a - a_0) + \alpha_h (h - h_0)], \quad (5)$$

where $R_{k,(\rho_0,h_0,a_0)} = 1.55 \times 10^{-9}$ m²K/W is the Kapitza resistance with no cross-linkers, reference overlap and normal distance ($a_0 = 40$ Å; $h_0 = 4$ Å), $\alpha_a = -0.034$ Å⁻¹ and $\alpha_h = 0.451$ Å⁻¹.

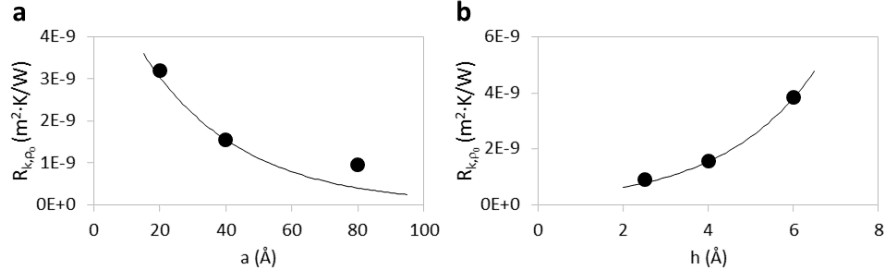


Figure 6: Thermal boundary resistance (R_k) at the GNR-GNR interface as a function of (a) horizontal overlap, a , and (b) normal distance, h , between nanoribbons. Molecular dynamics results (black dots) are fitted by the correlation reported in equation 5 (black curve).

4. Discussion

Effective medium theory (EMT) is a well-established theoretical framework for predicting a broad variety of properties of composite materials [58]. Among

others, electrical, mechanical, optical, and thermal properties of polymer based composites have been often interpreted by different implementations of EMT equations, with a good approximation of experimental results [59, 60].

According to Maxwell-Garnett formulation of EMT, the overall thermal conductivity of a composite material depends on the thermal conductivities of its constituents (matrix and filler) [58]. In general, the higher is the thermal conductivity of the filler (e.g. a sole GNR or a network of clustered GNRs), the higher is the effective thermal conductivity of the composite material. Hence, as the thermal conductivity of the GNR increases with its size (at least in the range 20–1000 nm), it is expected that also the overall thermal conductivity of the resulting composite material increases. Furthermore, Kapitza resistance at the interface between clustered GNRs should also play a significant role in determining the effective thermal conductivity of the composite material.

In order to better quantify the above hypothesis, a modified Maxwell-Garnett effective medium approximation is here considered. This model was first introduced by Shahil and Balandin [61] for graphene-polymer composites to take into account the filler-matrix Kapitza resistance (R_B):

$$\lambda_{eff} = \lambda_p \left[\frac{3\lambda_m + 2\phi(\lambda_p - \lambda_m)}{(3 - \phi)\lambda_p + \lambda_m\phi + \frac{R_B\lambda_m\lambda_p\phi}{H}} \right], \quad (6)$$

where λ_{eff} , λ_p and λ_m are thermal conductivities of composite, filler and matrix, respectively. Moreover, ϕ is the volume fraction of the filler and H is the filler thickness (0.35 nm in case of graphene monolayers). The model in equation 6 demonstrated good prediction capabilities for volume fractions lower than 15-20% and randomly oriented graphene based fillers [61].

Here, we consider the triple GNRs setup depicted in Fig. 1b as a representative building block of a filler network. By approximating the heat pathway through the filler as a 1D flow from the leftmost graphene sheet (GNR_L, with thermal conductivity λ_L and length $L_{x,L}$) to the middle (GNR_M, with thermal conductivity λ_M and length $L_{x,M}$) and finally to the rightmost one (GNR_R, with thermal conductivity λ_R and length $L_{x,R}$), the effective thermal resistance of the triple GNRs network can be roughly estimated as a series of lumped thermal

resistances, namely

$$\frac{L_p}{\lambda_p} = \frac{L_{x,L}}{\lambda_L} + R_{k,L} + \frac{L_{x,M}}{\lambda_M} + R_{k,R} + \frac{L_{x,R}}{\lambda_R}. \quad (7)$$

Clearly, different heat paths within the network may imply different estimates of the overall thermal resistance of the filler. In equation 7, L_p is the filler length, $R_{k,L}$ is the GNR_L-GNR_M Kapitza resistance while $R_{k,R}$ is the GNR_M-GNR_R one. The symmetry of the considered setup leads to $L_x = L_{x,L} = L_{x,M} = L_{x,R}$, $R_k = R_{k,L} = R_{k,R}$ and $\lambda = \lambda_L = \lambda_M = \lambda_R$; therefore, equation 7 can be simplified as

$$\lambda_p = \lambda \frac{3L_x}{3L_x + 2\lambda R_k}, \quad (8)$$

by considering the GNR-GNR overlap negligible respect to GNR length (i.e. $L_x \gg a$), which implies $L_p \cong 3L_x$.

The correlations found by atomistic experiments are then used to perform sensitivity analyses on the effect of GNR length, cross-linkers and relative arrangement on the effective thermal conductivity of polymer based composites, at least for volume fractions below the percolation threshold [62]. The aim is thus to provide some model-driven design guidelines for the synthesis of novel composite materials with enhanced thermal properties.

Based on the modified expression for the filler thermal conductivity in equation 8, the effect of GNR-GNR Kapitza resistance on the overall thermal conductivity of the nanocomposite is first studied by equation 6 (see Fig. 7a). In this analysis, ϕ ranges from 1% to 15%, while R_k varies from 1×10^{-11} to 1×10^{-8} m²K/W. Moreover, thermal conductivity of graphene (λ) is considered equal to 258 W/mK, which is the value measured by MD simulations for GNRs with 100 nm length, whereas $\lambda_m = 0.2$ W/mK [61, 63] and $R_B = 3.5 \times 10^{-9}$ m²K/W [61] are considered as average values of thermal conductivity and matrix-filler Kapitza resistance for the typical polymer matrices adopted in carbon based composite materials, respectively. Figure 7a highlights that the R_k effect on λ_{eff} is negligible for low volume concentrations of filler, while R_k plays a significant role on the resulting overall thermal conductivity of the nanocomposites for higher ϕ .

Moreover, thermal conductivities of nanocomposites with filler sizes ranging from 20 to 1000 nm and filler volume fractions from 1% to 15% are evaluated by equations 6 and 8 and plotted in Fig. 7b, while considering the R_k computed by MD in the triple GNR setup with no cross-linkers ($8.85 \times 10^{-10} \text{ m}^2\text{K/W}$). Results in Fig. 7b highlight a strong dependence of λ_{eff} with fillers length, at least with sub-micrometer graphene sheets. However, the absolute values of λ_{eff} may be strongly reduced in experimental conditions, because of the significant decrease in thermal conductivity driven by defects or vacancies in the graphene sheets [64, 65].

Finally, the effect of cross-linkers and relative arrangement between fillers on

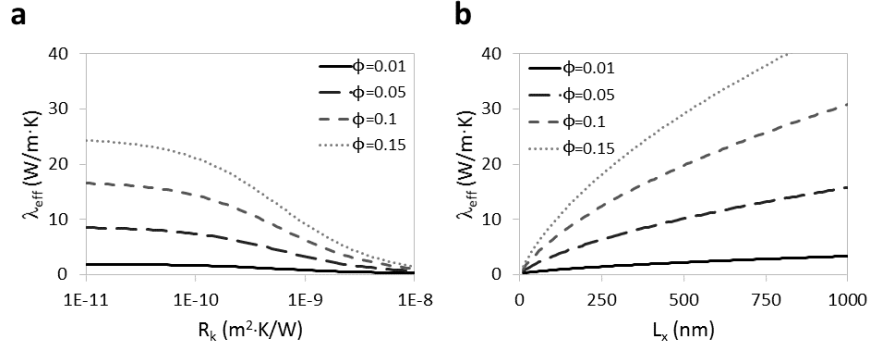


Figure 7: Predicted effective thermal conductivity of GNR-polymer nanocomposites. (a) Influence of GNR-GNR Kapitza resistance and volume concentration for GNRs with 100 nm length. (b) Influence of filler size and volume concentration, considering a fixed GNR-GNR Kapitza resistance of $8.85 \times 10^{-10} \text{ m}^2\text{K/W}$.

the effective thermal conductivity of polymer based composites is assessed. In fact, the correlations reported in equations 4 and 5 provide accurate bottom up values of R_k , which can be then adopted in the EMT model (equations 6 and 8) to estimate λ_{eff} with various filler characteristics. On the one side, Fig. 8a shows a direct exponential correlation between λ_{eff} and the overlap between GNR fillers (up to 5-fold increases in the considered a range); whereas, a more moderate correlation between λ_{eff} and the density of chemical cross-linkers at

the GNR-GNR interface is noticed in Fig. 8c (up to 2-fold increases in the considered ρ_{CL} range). On the other side, Fig. 8b depicts a strong inverse exponential correlation between λ_{eff} and the normal distance between contiguous nanofillers, with λ_{eff} decreasing up to 80% of its original value by only limited variations of h (5 Å).

Note that the calculated λ_{eff} are in the range of previously reported values for polymer matrix composites [66, 67, 68], therefore proving the qualitative validity of the methodology discussed in this work. Hence, by coupling nanoscale thermal properties of filler networks (obtained by atomistic simulations) with consolidated continuum models, the multiscale approach discussed in this work may represent an effective tool for performing sensitivity analyses on the effective properties of composite materials, as for example reported in Figs. 7 and 8 in case of GNR-polymer composites.

5. Conclusions

Computational materials science and engineering is emerging as a strongly interdisciplinary research field, with promising applications in the field of thermal sciences as well. In fact, materials research often needs a close interaction between experiments and computation to achieve a more fundamental understanding of materials properties and their relation to synthesis and processing. Especially in case of nanotechnology based materials, such as colloidal suspensions or composites filled by nanofibers, multiscale simulations, machine learning and data mining techniques have recently paved the way to discovering and designing new materials. In the near future, computational materials science is expected to lead to the reduction of materials development cost and time, the faster evolution of new materials into products and even the discovery of new materials [69].

Thanks to their peculiar light weight, mechanical strength and ease of process, the market is showing a growing interest for polymer based components in vari-

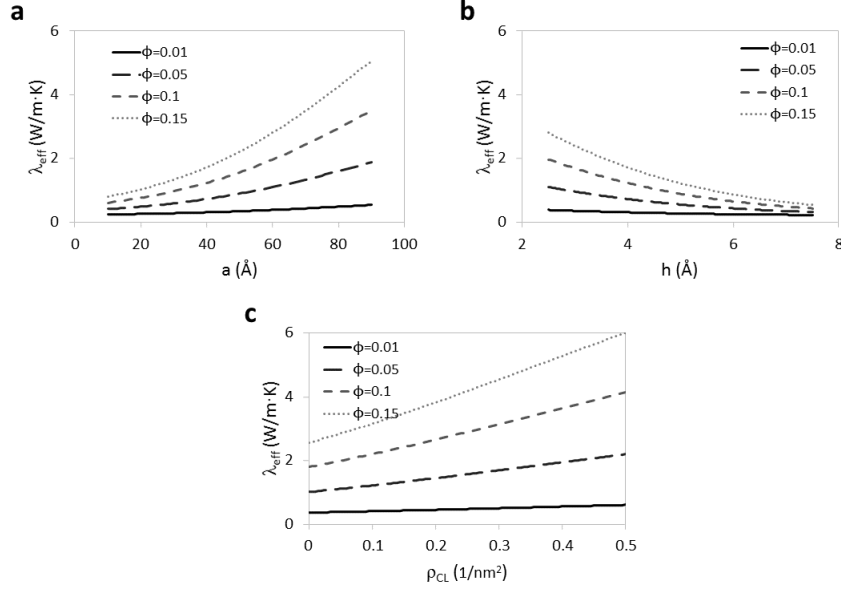


Figure 8: Effect of GNR-GNR relative orientation and functionalization on the effective thermal conductivity of polymer based composites. (a) Influence of GNR-GNR horizontal overlap and volume concentration of fillers, considering no cross-linkers. (b) Influence of GNR-GNR normal distance and volume concentration of fillers, considering no cross-linkers. (c) Influence of surface density of cross-linkers at the GNR-GNR interface, considering fixed $a = 4$ nm, $h = 0.25$ nm. In all cases, GNRs have 100 nm length and 2.4 nm width.

ous applications. However, due to the continuous progress in diverse industries, including energy, automotive, electronics and infrastructure sectors, and the demand for materials with higher performances, it is of great importance to improve the properties of polymer based composites by using fillers with superior properties. For instance, polymer based composites would need higher thermal conductivities in several applications, e.g. in heat exchange and thermal storage devices. To this purpose, nanometric fillers with high thermal conductivity (e.g. carbon nanotube or graphene) can be introduced in the polymeric matrix. Nevertheless, apart from the properties of matrix and filler, size and interfacial factors may strongly influence the overall thermal performance of the resulting composite material, and therefore should be mechanistically understood.

In the present work, RNEMD simulations are adopted to investigate the effect of filler size and thermal boundary resistance on the heat transfer within PMCs. Single GNR with length varying from 20 to 1000 nm and triple GNRs with either different orientation or surface density of cross-linkers have been studied. Simulation results show that thermal conductivity increases with GNR length, whereas thermal boundary resistance between overlapping GNRs can be reduced by either introducing covalent cross-links between fillers or by increasing their relative overlap and decreasing their normal distance. The reported correlations between fillers characteristics and their thermal properties allow then to predict the effective thermal transmittance of the network of fillers in the polymer matrix with a bottom up approach.

To analyze the effect of each of the latter factors on the overall thermal conductivity of PMC, simulation results are finally analyzed in the broader context of Maxwell-Garnett effective medium theory. PMCs with volume concentrations up to 15% are considered. It has been found that, at high volume concentrations, both GNR size and thermal boundary resistance between GNRs have significant effects on the overall thermal conductivity of PMC.

In conclusion, the multiscale approach and the correlations introduced in this article to quantitatively link atomistic results with macroscale properties of composites (i.e. effective thermal conductivity) can be adopted for a bottom up optimization of the thermal properties of filler networks. The aim is thus to provide guidelines for the computational discovery and rational design of nanofillers characteristics, in order to achieve polymer matrix composites with tunable thermal properties.

6. Appendix

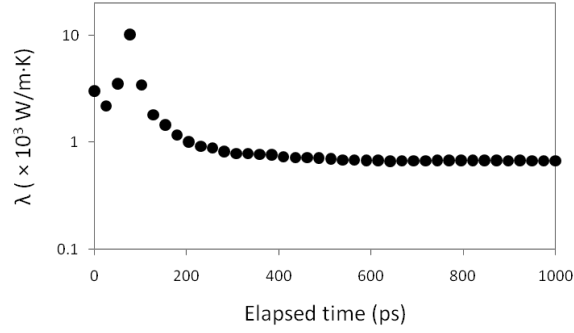


Figure A1: Convergence of the thermal conductivity of a simulated GNR ($L_x = 1000 \text{ nm}$) within the simulation time.

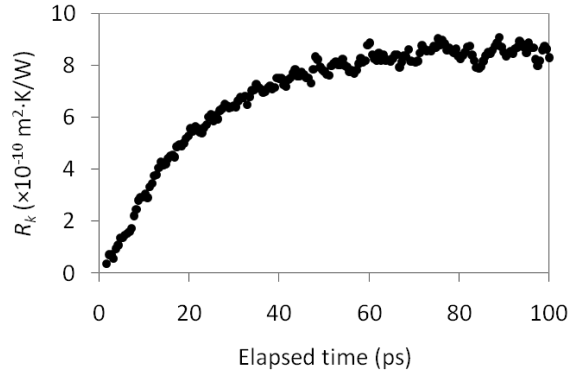


Figure A2: Convergence of thermal boundary resistance at the interface of contiguous GNRs ($a = 4 \text{ nm}$, $h = 0.25 \text{ nm}$, no cross-linkers) within the simulation time.

Competing interests

The authors declare that they have no competing interests.

Acknowledgments

Authors would like to acknowledge the NANO-BRIDGE – Heat and mass transport in NANO-structures by molecular dynamics, systematic model reduction, and non-equilibrium thermodynamics (PRIN 2012, grant number 2012LH-PSJC), the NANOSTEP – NANOfluid-based direct Solar absorption for Thermal Energy and water Purification (Fondazione CRT, Torino), and the DRAPO projects. Authors thank the CINECA (Iscra C projects COGRAINS) and the Politecnico di Torino’s DAUIN high-performance computing initiative for the availability of high-performance computing resources and support.

References

References

- [1] T. Skaltsas, N. Tagmatarchis, S. Pispas, Non-covalent graphene/polymer functional materials, *Current Organic Chemistry* 19 (18) (2015) 1800–1818.
- [2] F. Hussain, M. Hojjati, M. Okamoto, R. E. Gorga, Review article: polymer-matrix nanocomposites, processing, manufacturing, and application: an overview, *Journal of composite materials* 40 (17) (2006) 1511–1575.
- [3] E. Chiavazzo, P. Asinari, Reconstruction and modeling of 3d percolation networks of carbon fillers in a polymer matrix, *International Journal of Thermal Sciences* 49 (12) (2010) 2272–2281.
- [4] A. Gupta, S. Harsha, Studies of mechanical properties of multiwall nanotube based polymer composites, *Journal of Nanotechnology in Engineering and Medicine* 5 (3) (2014) 031006.
- [5] C. Koning, M.-C. Hermant, N. Grossiord, Polymer carbon nanotube composites: the polymer latex concept, Pan Stanford Publishing, 2012.
- [6] A. L. Pisello, A. D’Alessandro, S. Sambuco, M. Rallini, F. Ubertini, F. Asdrubali, A. L. Materazzi, F. Cotana, Multipurpose experimental characterization of smart nanocomposite cement-based materials for thermal-energy

- efficiency and strain-sensing capability, *Solar Energy Materials and Solar Cells* 161 (2017) 77–88.
- [7] M. J. Treacy, T. Ebbesen, J. Gibson, Exceptionally high young’s modulus observed for individual carbon nanotubes, *Nature* 381 (1996) 678–680.
 - [8] D. Chung, *Carbon Composites (Second Edition)*, Butterworth-Heinemann, 2017.
 - [9] A. M. Marconnet, M. A. Panzer, K. E. Goodson, Thermal conduction phenomena in carbon nanotubes and related nanostructured materials, *Reviews of Modern Physics* 85 (3) (2013) 1295.
 - [10] E. Chiavazzo, P. Asinari, Enhancing surface heat transfer by carbon nanofins: towards an alternative to nanofluids?, *Nanoscale research letters* 6 (1) (2011) 1–13.
 - [11] E. Chiavazzo, M. Fasano, P. Asinari, P. Decuzzi, Scaling behaviour for the water transport in nanoconfined geometries, *Nature communications* 5 (2014) 4565.
 - [12] M. Fasano, E. Chiavazzo, P. Asinari, Water transport control in carbon nanotube arrays, *Nanoscale research letters* 9 (1) (2014) 1–8.
 - [13] M. B. Bigdeli, M. Fasano, A. Cardellini, E. Chiavazzo, P. Asinari, A review on the heat and mass transfer phenomena in nanofluid coolants with special focus on automotive applications, *Renewable and Sustainable Energy Reviews* 60 (2016) 1615–1633.
 - [14] Z. Han, A. Fina, Thermal conductivity of carbon nanotubes and their polymer nanocomposites: a review, *Progress in polymer science* 36 (7) (2011) 914–944.
 - [15] M. Fasano, D. Borri, E. Chiavazzo, P. Asinari, Protocols for atomistic modeling of water uptake into zeolite crystals for thermal storage and other applications, *Applied Thermal Engineering* 101 (2016) 762–769.

- [16] J. E. Peters, D. V. Papavassiliou, B. P. Grady, Unique thermal conductivity behavior of single-walled carbon nanotube-polystyrene composites, *Macromolecules* 41 (2008) 7274–7277.
- [17] U. A. Joshi, S. C. Sharma, S. Harsha, Influence of dispersion and alignment of nanotubes on the strength and elasticity of carbon nanotubes reinforced composites, *Journal of Nanotechnology in Engineering and Medicine* 2 (4) (2011) 041007.
- [18] T. Luo, J. R. Lloyd, Enhancement of thermal energy transport across graphene/graphite and polymer interfaces: a molecular dynamics study, *Advanced Functional Materials* 22 (12) (2012) 2495–2502.
- [19] P. D. Gujrati, A. I. Leonov, *Modeling and Simulation in Polymers*, John Wiley & Sons, 2010.
- [20] T. C. Clancy, S.-J. V. Frankland, J. A. Hinkley, T. S. Gates, Multiscale modeling of thermal conductivity of polymer/carbon nanocomposites, *International Journal of Thermal Sciences* 49 (9) (2010) 1555–1560.
- [21] C. Yuan, L. Li, B. Duan, B. Xie, Y. Zhu, X. Luo, Locally reinforced polymer-based composites for efficient heat dissipation of local heat source, *International Journal of Thermal Sciences* 102 (2016) 202–209.
- [22] X. Huang, P. Jiang, T. Tanaka, A review of dielectric polymer composites with high thermal conductivity, *Electrical Insulation Magazine*, IEEE 27 (4) (2011) 8–16.
- [23] H. Qian, E. S. Greenhalgh, M. S. Shaffer, A. Bismarck, Carbon nanotube-based hierarchical composites: a review, *Journal of Materials Chemistry* 20 (23) (2010) 4751–4762.
- [24] M. A. Worsley, P. J. Pauzauskie, T. Y. Olson, J. Biener, J. H. Satcher Jr, T. F. Baumann, Synthesis of graphene aerogel with high electrical conductivity, *Journal of the American Chemical Society* 132 (40) (2010) 14067–14069.

- [25] M. Fasano, M. B. Bigdeli, M. R. V. Sereshk, E. Chiavazzo, P. Asinari, Thermal transmittance of carbon nanotube networks: guidelines for novel thermal storage systems and polymeric material of thermal interest, *Renewable and Sustainable Energy Reviews* 41 (2015) 1028–1036.
- [26] S. Shenogin, A. Bodapati, L. Xue, R. Ozisik, P. Keblinski, Effect of chemical functionalization on thermal transport of carbon nanotube composites, *Applied Physics Letters* 85 (12) (2004) 2229–2231.
- [27] B. Mortazavi, O. Benzerara, H. Meyer, J. Bardon, S. Ahzi, Combined molecular dynamics-finite element multiscale modeling of thermal conduction in graphene epoxy nanocomposites, *Carbon* 60 (2013) 356–365.
- [28] D. Konatham, A. Striolo, Thermal boundary resistance at the graphene-oil interface, *Applied Physics Letters* 95 (16) (2009) 163105.
- [29] V. Varshney, S. S. Patnaik, A. K. Roy, B. L. Farmer, Modeling of thermal conductance at transverse cnt-cnt interfaces, *The Journal of Physical Chemistry C* 114 (39) (2010) 16223–16228.
- [30] M. Wang, N. Hu, L. Zhou, C. Yan, Enhanced interfacial thermal transport across graphene–polymer interfaces by grafting polymer chains, *Carbon* 85 (2015) 414–421.
- [31] J. Chen, J. H. Walther, P. Koumoutsakos, Strain engineering of kapitza resistance in few-layer graphene, *Nano letters* 14 (2) (2014) 819–825.
- [32] H. Tomita, J. Nakamura, Ballistic phonon thermal conductance in graphene nanoribbons, *Journal of Vacuum Science & Technology B, Nanotechnology and Microelectronics: Materials, Processing, Measurement, and Phenomena* 31 (4) (2013) 04D104.
- [33] F. Müller-Plathe, A simple nonequilibrium molecular dynamics method for calculating the thermal conductivity, *The Journal of chemical physics* 106 (14) (1997) 6082–6085.

- [34] S. Plimpton, Fast parallel algorithms for short-range molecular dynamics, *Journal of computational physics* 117 (1) (1995) 1–19.
- [35] D. W. Brenner, O. A. Shenderova, J. A. Harrison, S. J. Stuart, B. Ni, S. B. Sinnott, A second-generation reactive empirical bond order (rebo) potential energy expression for hydrocarbons, *Journal of Physics: Condensed Matter* 14 (4) (2002) 783.
- [36] N. Wei, L. Xu, H.-Q. Wang, J.-C. Zheng, Strain engineering of thermal conductivity in graphene sheets and nanoribbons: a demonstration of magic flexibility, *Nanotechnology* 22 (10) (2011) 105705.
- [37] V. Varshney, S. S. Patnaik, A. K. Roy, G. Froudakis, B. L. Farmer, Modeling of thermal transport in pillared-graphene architectures, *ACS nano* 4 (2) (2010) 1153–1161.
- [38] T. Ng, J. Yeo, Z. Liu, A molecular dynamics study of the thermal conductivity of graphene nanoribbons containing dispersed stone–thrower–wales defects, *Carbon* 50 (13) (2012) 4887–4893.
- [39] C.-A. Palma, M. Awasthi, Y. Hernandez, X. Feng, K. Müllen, T. A. Niehaus, J. V. Barth, Sub-nanometer width armchair graphene nanoribbon energy gap atlas, *The Journal of Physical Chemistry Letters* 6 (16) (2015) 3228–3235.
- [40] D. Goyal, S. Kumar, A. Shukla, R. Kumar, Origin of multiple band gap values in single width nanoribbons, *Scientific reports* 6 (2016) 36168.
- [41] R. M. Jacobberger, B. Kiraly, M. Fortin-Deschenes, P. L. Levesque, K. M. McElhinny, G. J. Brady, R. R. Delgado, S. S. Roy, A. Mannix, M. G. Lagally, et al., Direct oriented growth of armchair graphene nanoribbons on germanium, *Nature communications* 6 (2015) 8006.
- [42] X. Li, X. Wang, L. Zhang, S. Lee, H. Dai, Chemically derived, ultra-smooth graphene nanoribbon semiconductors, *Science* 319 (5867) (2008) 1229–1232.

- [43] A. Bagri, S.-P. Kim, R. S. Ruoff, V. B. Shenoy, Thermal transport across twin grain boundaries in polycrystalline graphene from nonequilibrium molecular dynamics simulations, *Nano letters* 11 (9) (2011) 3917–3921.
- [44] P. K. Schelling, S. R. Phillpot, P. Keblinski, Comparison of atomic-level simulation methods for computing thermal conductivity, *Physical Review B* 65 (14) (2002) 144306.
- [45] Z. Guo, D. Zhang, X.-G. Gong, Thermal conductivity of graphene nanoribbons, *Applied physics letters* 95 (16) (2009) 163103.
- [46] P. Rui-Qin, X. Zi-Jian, Z. Zhi-Yuan, Length dependence of thermal conductivity of single-walled carbon nanotubes, *Chinese Physics Letters* 24 (5) (2007) 1321.
- [47] S. Ghosh, I. Calizo, D. Teweldebrhan, E. Pokatilov, D. Nika, A. Balandin, W. Bao, F. Miao, C. N. Lau, Extremely high thermal conductivity of graphene: Prospects for thermal management applications in nanoelectronic circuits, *Applied Physics Letters* 92 (15) (2008) 151911.
- [48] J. Hu, X. Ruan, Y. P. Chen, Thermal conductivity and thermal rectification in graphene nanoribbons: a molecular dynamics study, *Nano letters* 9 (7) (2009) 2730–2735.
- [49] X. Xu, L. F. Pereira, Y. Wang, J. Wu, K. Zhang, X. Zhao, S. Bae, C. T. Bui, R. Xie, J. T. Thong, et al., Length-dependent thermal conductivity in suspended single-layer graphene, *Nature communications* 5 (2014) 3689.
- [50] E. Pop, V. Varshney, A. K. Roy, Thermal properties of graphene: Fundamentals and applications, *MRS bulletin* 37 (12) (2012) 1273–1281.
- [51] D. Bullett, Chemical pseudopotential approach to covalent bonding. ii. bond lengths and bond energies in diamond, silicon and graphite, *Journal of Physics C: Solid State Physics* 8 (17) (1975) 2707.

- [52] S. J. Stuart, A. B. Tutein, J. A. Harrison, A reactive potential for hydrocarbons with intermolecular interactions, *The Journal of chemical physics* 112 (14) (2000) 6472–6486.
- [53] M. C. Schabel, J. L. Martins, Energetics of interplanar binding in graphite, *Physical Review B* 46 (11) (1992) 7185.
- [54] Z. Chen, W. Ren, L. Gao, B. Liu, S. Pei, H.-M. Cheng, Three-dimensional flexible and conductive interconnected graphene networks grown by chemical vapour deposition, *Nature materials* 10 (6) (2011) 424–428.
- [55] A. Aitkaliyeva, D. Chen, L. Shao, Phonon transport assisted by inter-tube carbon displacements in carbon nanotube mats, *Scientific reports* 3 (2013) 2774.
- [56] X. Tian, M. L. Moser, A. Pekker, S. Sarkar, J. Ramirez, E. Bekyarova, M. E. Itkis, R. C. Haddon, Effect of atomic interconnects on percolation in single-walled carbon nanotube thin film networks, *Nano letters* 14 (7) (2014) 3930–3937.
- [57] E. T. Swartz, R. O. Pohl, Thermal boundary resistance, *Reviews of modern physics* 61 (3) (1989) 605.
- [58] T. C. Choy, *Effective medium theory: principles and applications*, Oxford University Press, 2015.
- [59] P. Hui, X. Zhang, A. Markworth, D. Stroud, Thermal conductivity of graded composites: Numerical simulations and an effective medium approximation, *Journal of materials science* 34 (22) (1999) 5497–5503.
- [60] K. Wu, Y. Xue, W. Yang, S. Chai, F. Chen, Q. Fu, Largely enhanced thermal and electrical conductivity via constructing double percolated filler network in polypropylene/expanded graphite–multi-wall carbon nanotubes ternary composites, *Composites Science and Technology* 130 (2016) 28–35.

- [61] K. M. Shahil, A. A. Balandin, Graphene-multilayer graphene nanocomposites as highly efficient thermal interface materials, *Nano letters* 12 (2) (2012) 861–867.
- [62] J. Li, J.-K. Kim, Percolation threshold of conducting polymer composites containing 3d randomly distributed graphite nanoplatelets, *Composites Science and Technology* 67 (10) (2007) 2114–2120.
- [63] H. Chen, V. V. Ginzburg, J. Yang, Y. Yang, W. Liu, Y. Huang, L. Du, B. Chen, Thermal conductivity of polymer-based composites: Fundamentals and applications, *Progress in Polymer Science* 59 (2016) 41–85.
- [64] F. Hao, D. Fang, Z. Xu, Mechanical and thermal transport properties of graphene with defects, *Applied physics letters* 99 (4) (2011) 041901.
- [65] K. Yuan, M. Sun, Z. Wang, D. Tang, Tunable thermal rectification in silicon-functionalized graphene nanoribbons by molecular dynamics simulation, *International Journal of Thermal Sciences* 98 (2015) 24–31.
- [66] L. M. Veca, M. J. Meziani, W. Wang, X. Wang, F. Lu, P. Zhang, Y. Lin, R. Fee, J. W. Connell, Y.-P. Sun, Carbon nanosheets for polymeric nanocomposites with high thermal conductivity, *Advanced Materials* 21 (20) (2009) 2088–2092.
- [67] A. Yu, P. Ramesh, M. E. Itkis, E. Bekyarova, R. C. Haddon, Graphite nanoplatelet-epoxy composite thermal interface materials, *The Journal of Physical Chemistry C* 111 (21) (2007) 7565–7569.
- [68] N. K. Mahanta, M. R. Loos, I. M. Zloczower, A. R. Abramson, Graphite–graphene hybrid filler system for high thermal conductivity of epoxy composites, *Journal of Materials Research* 30 (07) (2015) 959–966.
- [69] L.-Q. Chen, L.-D. Chen, S. V. Kalinin, G. Klimeck, S. K. Kumar, J. Neugebauer, I. Terasaki, Design and discovery of materials guided by theory and computation, *npj Computational Materials* 1 (2015) 15007.